# Prokaryotic Expression of the Heme- and Flavin-Binding Domains of Rat Neuronal Nitric Oxide Synthase as Distinct Polypeptides: Identification of the Heme-Binding Proximal Thiolate Ligand as Cysteine-415†

Kirk McMillan and Bettie Sue Siler Masters*

*Department of Biochemistry, University of Texas Health Science Center at San Antonio, San Antonio, Texas 78284-7760*

*Received September 2, 1994; Revised Manuscript Received December 1, 1994*®

ABSTRACT: The heme- and flavin-binding domains of constitutive rat neuronal nitric oxide synthase (NOS) were expressed in *Escherichia coli* as distinct polypeptides with properties characteristic of the intact enzyme. The amino-terminal heme-binding domain (residues 1−714) was expressed using the expression vector pCW. The denatured molecular mass of the expressed protein was 80 kDa, and the protein was shown to be immunoreactive to rabbit anti-NOS IgG. The NOS hemoprotein exhibited a ferrous-carbon monoxide difference spectrum with a wavelength maximum at 445 nm. Spectral perturbation with L-arginine and $BH_4$ elicited a type I difference spectrum, confirming the presence of binding sites for these molecules within the N-terminal NOS polypeptide. Site-directed mutagenesis was applied to the putative axial heme ligand, cysteine-415, generating the histidine mutant, which confirmed the identity of the proximal ligand. NOS flavoproteins, with (C1, residues 715−1429) and without (C2, residues 749−1429) an amino-terminal calmodulin-binding motif, were expressed using the vector pPROK-1. The C1 and C2 flavoproteins were immunoreactive to anti-NOS IgG and were sized at approximately 80 kDa. Both of the purified flavoproteins exhibited optical absorbance properties typical of a flavin prosthetic group, with wavelength maxima at 380 and 450 nm, and were competent in NADPH-dependent electron transfer to cytochrome *c*, with observed rates of ~2−4 μmol/min/mg. The bacterial expression of the NO synthase heme-binding oxygenase and flavoprotein oxidoreductase domains as isolated proteins with specific properties of the intact enzyme represents an important development in structure−function studies of this complex enzyme.

Nitric oxide synthases (NOSs)[1] constitute a family of enzymes that catalyze the NADPH-dependent conversion of L-arginine to nitric oxide and L-citrulline. NO synthases are >130-kDa polypeptides containing iron protoporphyrin IX (White & Marletta, 1992; Stuehr & Ikeda-Saito, 1992; McMillan *et al.,* 1992; Klatt, *et al.,* 1992), FAD, and FMN (Stuehr *et al.,* 1991a; Bredt *et al.,* 1992) prosthetic groups and tetrahydrobiopterin (Mayer *et al.,* 1991). The metabolism of the substrate, L-arginine, occurs through two subsequent monooxygenation reactions utilizing molecular oxygen (Kwon *et al.,* 1990) in which the heme iron serves as the reaction center. The constitutive, soluble neuronal (Bredt *et al.,* 1990) and particulate endothelial (Pollock *et al.,* 1991) NOS isoforms are calcium/calmodulin-dependent, while the transcriptionally regulated macrophage enzyme binds calmodulin as a subunit independent of calcium (Cho *et al.,* 1992). Furthermore, electron flow from NADPH via the carboxy-terminal flavoprotein has been shown to be a calcium/calmodulin-dependent process (Abu-Soud & Stuehr, 1993). Bredt and colleagues (1991) reported 36% identity and 58% sequence similarity within the C-terminal 641 amino acid residues of rat neuronal NOS to rat liver NADPH−cytochrome P450 oxidoreductase and identified conserved sites for FAD, FMN, and NADPH binding. Residues 725−745 were also proposed to function as the calmodulin-binding motif (Bredt *et al.,* 1991), which was subsequently confirmed by peptide competition experiments (Vorherr *et al.,* 1993) and supported by trypsinolysis studies of Sheta *et al.,* (1994). The assignment of the heme-binding region to the N-terminal domain was made by inspection of the amino acid sequences of rat neuronal, murine macrophage, and bovine endothelial enzymes in which highly conserved cysteinyl peptides (*e.g.*, rat neuronal: WRNSRCVRGIQW) were observed within the amino-terminal domains (McMillan *et al.,* 1992). Although the NOS peptide sequence possesses marked differences from the consensus cytochrome P450 cysteinyl peptide, FXXGXXXCCXG, comparison to mammalian cytochromes P450 putative cysteinyl peptides, such as that of rat $P450_d$, FGLGKRRC$_{456}$IGEI (Shimizu *et al.,* 1988), shows the conservation of several hydrophobic residues, glycine(s), and an arginine. Thus, the respective cysteine residue, specifically cysteine-415 for rat neuronal NOS, has been suggested by McMillan *et al.* (1992) to serve in the ligation of the heme iron at the proximal axial site (*vide infra*). In the present paper, site-directed mutagenesis of the cysteine to histidine was used to verify the identity of the heme proximal ligand. Limited

† Supported by The Robert A. Welch Foundation Grant AQ-1192 and, in part, by NIH Grant HL30050. K.M. is a Predoctoral Fellow of The Robert A. Welch Foundation.

* To whom correspondence should be addressed.

® Abstract published in *Advance ACS Abstracts,* March 1, 1995.

[1] Abbreviations: δ-ALA, δ-aminolevulinic acid; 2′-AMP, 2′-adenosine monophosphate; BME, β-mercaptoethanol; dNTPs, deoxynucleotide triphosphates; EDTA, ethylenediaminetetraacetic acid; EGTA, ethylene glycol bis(β-aminoethyl ether)-*N,N,N′,N′*-tetraacetic acid; FAD, flavin adenine dinucleotide; FMN, flavin mononucleotide; NADPH, nicotinamide adenine dinucleotide phosphate; Ni-NTA, nickel nitrilotriacetic acid; NOS, nitric oxide synthase; PMSF, phenylmethanesulfonyl fluoride; SDS−PAGE, sodium dodecyl sulfate−polyacrylamide gel electrophoresis.

0006-2960/95/0434-3686$09.00/0 

Table 1: Oligonucleotide Primers

| primer | sequence |
|---|---|
| N1 | AAGGACACAGATCATATGGAAGAGAACACG |
| N2 | TTCGTGGGGGTCCCGTTGGTAAGCTTTTACACGTGGGTGTTCCA |
| N3 | GACACAGATACCCATATGGCA[CAC]$_4$GAAGAGAACACGTTTGGG |
| C1 | CTGAAGGACACAGAATTCATGGTGTGGAAGGGC |
| C2 | AAGCTAATGGGGGAATTCATGGCCAAGAGG |
| C3 | ACGCACGGGGGCAGGAGGGAATTCTTAGGAGCTGAAAAC |
| H1 | ACCGAGCTCATCTATGGCGCC |
| H2 | TGGGGCTTTCCAGCCCTGCTG |
| CH | pCGCCTCTCGATCTGTGGGCAGG |

proteolysis of rat neuronal NOS has recently confirmed the bidomain nature of the enzyme (Sheta *et al.*, 1994), which led to a proposed structure composed of an amino-terminal heme-binding oxygenase and a carboxy-terminal flavoprotein oxidoreductase connected by a central calmodulin-binding motif. The FAD- and FMN-containing flavoprotein serves in the calmodulin-modulated transfer of single electrons from the two-electron source, NADPH, to the heme iron reaction center. Recently, the position of the putative pterin-binding domain, within residues 558−720, was assigned by sequence comparison to dihydrofolate reductases for which the crystal structures are known (Salerno & Morales, 1994).

The 119-kDa fatty acid hydroxylase cytochrome P450$_{BM-3}$ of *Bacillus megaterium* was shown to possess an analogous bidomain structure (Nahri & Fulco, 1987), which was successfully resolved into its component parts by molecular cloning methods (Li *et al.*, 1991). Reconstitution of fatty acid hydroxylation by the recombinant cytochrome P450$_{BM-3}$ domains was obtained by Boddupalli *et al.* in 1992, and the high-resolution crystal structure of the heme-binding oxygenase domain was recently reported (Ravichandran *et al.*, 1993), thus providing further support for the experimental approach of resolving NO synthase into its functional modules as reported herein.

The work reported here supports a hypothesis that NO synthases are the result of evolutionary gene fusion that formed a series of functional modules aligned within the linear protein sequence, *i.e.*, the fusion of the heme-binding oxygenase with the flavoprotein oxidoreductase by a connecting modulatory sequence. The following scheme depicts the proposed modular structure of neuronal NOS.

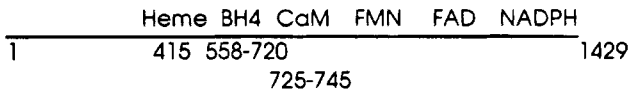


These domains possess unique tertiary structures, independent of residues within the adjacent domains, which dictate the function of the respective domain. The availability of the isolated catalytic domains of neuronal NOS for characterization will facilitate the understanding of the mechanism of substrate oxygenation and may ultimately lead to the elucidation of the three-dimensional structure of this important enzyme.

## EXPERIMENTAL PROCEDURES

The plasmids pNOS, containing the rat neuronal constitutive NOS cDNA in pBluescript SK(−), and pNOS 64, containing the coding region for the C-terminal 714 amino acids, were generously provided by Drs. Solomon Snyder and David Bredt at Johns Hopkins Medical School, Baltimore, MD (Bredt *et al.*, 1991). The expression vectors (*tac* promoter) pCWori+ (Gegner & Dahlquist, 1991) and pPROK-1 (Clonetech, Palo Alto, CA) were used for the hemoprotein and flavoproteins, respectively. Oligonucleotides were synthesized by the Department of Medicine Biopolymer Facility and The Center for Advanced DNA Technologies at The University of Texas Health Science Center at San Antonio and are described in Table 1. Taq DNA polymerase was obtained from Promega, Cambridge, MA. Taq DNA ligase and other enzymes used in molecular biology were obtained from New England Biolabs, Boston, MA. Competent *Escherichia coli* JM109 cells were from Stratagene, La Jolla, CA. Ni-NTA agarose was obtained from Qiagen, Chatsworth, CA.

*Molecular Biology.* The plasmid for the expression of the nNOS heme-binding domain was made as follows. Polymerase chain reaction-mediated amplification of nucleotides 349−2490 with *NdeI*/*Hin*dIII restriction sites was performed using pNOS as the template and the N1 (upstream) and N2 (downstream) primer set (see Table 1). Reaction mixtures contained 50 pmol of each primer, 200 $\mu$M dNTPs, 1 mM $MgCl_2$, 1× Taq polymerase buffer, and 2−3 units of Taq polymerase in 50 mL. The temperature cycling conditions were 60 s at 94, 55, and 72 °C, repeated for 25 cycles. The amplified products were recovered by band excision, digested with *NdeI*/*Hin*dIII, and ligated to restricted pCW. *E. coli* JM109 cells were transformed with the resultant ligation products and plated on LB agar containing 50 mg/L ampicillin. Recombinant colonies were screened by restriction mapping. Three positive clones were screened for IPTG-induced protein expression by SDS−polyacrylamide gel electrophoresis and immunoblot analysis using rabbit anti-rat recombinant neuronal NOS IgG. The DNA sequence of the PCR-amplified insert was confirmed by automated dideoxy sequencing using an Applied Biosystems 373A DNA sequencer and fluorescence-labeled dideoxynucleotides. PCR amplification, using the N2/N3 primer set of an *NdeI*/*Hin*dIII fragment encoding an amino-terminal histidine$_4$-tagged hemoprotein, and ligation into pCW were performed, employing identical methods.

Similar methods were used in the preparation of the pPROK-1 constructs containing *Eco*RI inserts corresponding to nucleotides 2491−4635 and 2593−4635 for the expression of the C1 (residues 715−1429) and C2 (residues 749−1429) flavoproteins, respectively. The oligonucleotide primers used in the amplification of the respective inserts were C1 or C2 (upstream) and C3 (downstream). The plasmid pNOS 64 was used as the template. The nucleotide sequence of the insert for each of the final clones was confirmed by dideoxy sequencing as described above.

*Site-Directed Mutagenesis of Cysteine-415.* The putative cysteinyl peptide is encoded within the NOS cDNA by a 304-bp segment which is flanked by unique *Nar*I and *Bst*1107I restriction sites. Coincident amplification of the *Nar*I/*Bst*1107I fragment and incorporation of a mutagenic phosphorylated oligonucleotide was obtained by using Taq DNA polymerase and Taq ligase in thermal cycle reactions (Michael, 1994). The following primers were used: H1, H2, and phosphorylated CH. Reaction mixtures contained 200 pmol of each primer, 400 $\mu$M dNTPs, 1× Taq ligase buffer, 5 units of Taq DNA polymerase, and 40 units of Taq DNA ligase in a final volume of 100 mL. Thermal cycles were as follows: one cycle, 94 °C/5 min, 50 °C/1 min, and 65 °C/4 min; and 29 cycles, 94 °C/30 s, 50 °C/1 min, and 65 °C/4 min. Reaction products were recovered by band excision, restricted with *Nar*I/*Bst*1107I, and ligated into restricted pNOS. Clones were screened for the presence of the *Nar*I/*Bst*1107I insert. The $\Delta CH^{415}$ mutagenesis resulted in the generation of a novel *Afl*III site at nucleotide 1591 which was used in screening. Positive clones were subsequently amplified by PCR using the N2/N3 primer set for expression in the $His_4$-tagged system to allow protein purification by Ni-chelate chromatography. The PCR reaction conditions were the same as those employed in the generation of the original hemoprotein-encoding *Nde*I/*Hin*dIII fragment. The amplified nucleotide sequence encoding the mutant hemoprotein was confirmed by automated dideoxy sequencing.

*Protein Expression.* Cell culture was performed in Fernbach flasks containing 1 L of modified Terrific Broth (10 g/L tryptone, 20 g/L yeast extract, 4 mL/L glycerol, 19.5 mM $KH_2PO_4$, and 30.5 mM $Na_2HPO_4$) with 50 mg/L of ampicillin. Cultures were incubated at 30 and 37 °C for the flavoproteins and hemoproteins, respectively. Culture aeration was provided by shaking the Fernbach flasks at 250 rev/min. Protein expression was induced at an optical density of ~0.8−1.2 at 600 nm by addition of 1 mM IPTG. In addition, the heme and flavin biosynthetic precursors $\delta$-ALA (0.2 mM) and riboflavin (1−3 $\mu$M), respectively, were added at the time of induction to the respective cultures. Cells were harvested (17−18 h post-induction for the hemoprotein and 36 h for the flavoprotein) by centrifugation and frozen at −80 °C.

*Hemoprotein Purification.* The frozen cells (from 10 L of culture) were thawed in approximately 3−4 vol of buffer A (50 mM Tris-HCl, 5 mM EDTA, 1 mM PMSF, 1 mM EGTA, 1 mM BME, 5 $\mu$g/mL leupeptin/pepstatin, and 200 mg/mL lysozyme, pH 7.5). The cells were lysed by pulsed sonication for 5 min and centrifuged at 18000*g* for 20 min. The supernatant was then centrifuged at 100000*g* for 60 min. Glycerol was added to the supernatant to a final concentration of 10% (v/v). The solution was adjusted to 55% saturated ammonium sulfate by the addition of saturated, neutral $(NH_4)_2SO_4$ solution and stirred for 1 h. The precipitate was collected by centrifugation at 18000*g* for 30 min. The precipitate was dissolved in 100 mL of buffer B (20 mM Tris-HCl, 10% glycerol, 1 mM BME, 0.2 mM PMSF, and 1 $\mu$g/mL leupeptin/pepstatin, pH 7.5) and dialyzed overnight against 4 L of buffer B. The dialysate was applied to a 40-mL column of Q Sepharose equilibrated with buffer B. The column was washed with 100 mL of buffer B and eluted with a 400-mL gradient from 0 to 0.5 M NaCl in buffer B. Fractions (5 mL) were pooled according to absorbance at 405 nm. Immunoblot and spectral analyses of hemoprotein purified as described above are shown in Figures 1 and 2, respectively. All manipulations in the purification of the hemo- and flavoproteins were conducted at 4 °C.

*Flavoprotein Purification.* The flavoproteins were purified from a soluble extract, prepared as described above (cell paste from 4 L of culture). The protein extract was loaded onto 25 ml of 2′,5′-ADP Sepharose equilibrated with buffer B. The column was washed sequentially with 200 mL of 0.2 M NaCl in buffer B, 100 mL of buffer B, 1 mM adenosine and 1 mM 2′-AMP in buffer B, and finally 200 mL of buffer B. The flavoprotein was then eluted with 100 mL of 5 mM 2′-AMP and 0.5 M NaCl in buffer B, and fractions (2 mL) were pooled on the basis of the flavin absorbance at 450 nm. The calmodulin-binding C1 flavoprotein was further purified by calmodulin affinity chromatography. $CaCl_2$ was added to a final concentration of 2 mM, and the mixture was applied to a 5-mL calmodulin agarose:Sepharose 4B (1:8) column equilibrated with buffer B containing 2 mM $CaCl_2$ (buffer C). The column was washed with 100 mL of buffer C and 25 mL of 0.2 M NaCl in buffer C. Protein was eluted with 5 mM EGTA and 0.5 M NaCl in buffer B and concentrated by ultrafiltration using a Centriprep 30. The concentrate was oxidized by the addition of a few grains of solid potassium ferricyanide and was then desalted by Sephadex G50 chromatography using buffer B without BME. The C2 flavoprotein was subjected to 2′,5′-ADP Sepharose chromatography as described above. The pooled fractions were dialyzed against buffer B and applied to 20 mL of DEAE Sepharose CL6B equilibrated with buffer B. The column was washed with 60 mL of buffer B and eluted with a 200-mL linear gradient from 0 to 0.5 M NaCl in buffer B. Fractions (2 mL) were pooled on the basis of absorbance at 450 nm and concentrated by ultrafiltration. The protein concentrate was applied to a 1.5 × 90 cm column of Sephacryl 200 equilibrated with buffer D (50 mM Tris-HCl, 10% glycerol, 0.1 M NaCl, 0.1 mM EDTA, 0.2 mM PMSF, and 1 $\mu$g/mL leupeptin/pepstatin, pH 7.5). Fractions (2 mL) were pooled by flavin absorbance as described.

*Purification of $His_4$-Hemoproteins.* Frozen cells (from 4 L of culture) were thawed in 3 vol of 50 mM Tris-HCl, 10% glycerol, 5 mM EDTA, 5 mM BME, 1 mM EGTA, 1 mM PMSF, and 5 $\mu$g/mL leupeptin/pepstatin containing 200 $\mu$g/mL lysozyme. The cell suspension was sonicated for 5 min and centrifuged as described above to prepare a clarified cell extract. The hemoprotein-containing extract was then subjected to ammonium sulfate precipitation as described. The precipitant was dissolved in 50 mL of 50 mM $NaP_i$, 10% glycerol, 0.2 M NaCl, 1 mM BME, 0.2 mM PMSF, and 1 $\mu$g/mL leupeptin/pepstatin, pH 7.8, and dialyzed against 4 L of the same buffer. The dialyzed sample was clarified by centrifugation for 30 min at 18000*g*, and 100 mM imidazole, pH 7.8, was added to a final concentration of 10 mM. The sample was applied to a 3-mL column of Ni-NTA agarose equilibrated with the $NaP_i$ buffer containing 10 mM imidazole. The column was washed with 30 mL of 50 mM $NaP_i$, 10% glycerol, 0.4 M NaCl, 20 mM imidazole, 5 mM BME, 0.2 mM PMSF, and 1 $\mu$g/mL leupeptin/pepstatin, pH 7.8. The column was then eluted with 50 mM $NaP_i$, 10% glycerol, 0.2 M NaCl, 100 mM imidazole, 1 mM BME, 0.2 mM PMSF, and 1 $\mu$g/mL leupeptin/pepstatin, pH 7.8. Fractions (1 mL) were pooled by absorbance of the heme Soret transition band and were dialyzed against buffer B to remove

the imidazole.

*Optical Spectroscopy.* Spectrophotometric measurements were performed using a Shimadzu 2101 dual-beam spectrophotometer. Formation of the hemoprotein ferrous-CO adduct, with a Soret band at 445 nm, was used to quantitate the hemoprotein. Samples were bubbled with CO for 5−10 s and divided between the sample and reference cuvettes. The absorbance difference was adjusted to zero, and the contents of the sample cuvette were reduced by addition of a few grains of solid sodium dithionite. The difference spectrum was recorded from 500 to 400 nm, and the concentration of the target hemoprotein was estimated using the extinction coefficient ~75 mM $^{-1}$ ($A_{445}-A_{470}$). This extinction coefficient (75 $mM^{-1}$) was also used in the estimation of hemoprotein from the Soret transition band absorbance and the L-arginine difference spectra. Stuehr and Ikeda-Saito (1992) reported extinction coefficients of $\epsilon_{397}$ = 72 $mM^{-1}$ for ferric nNOS and $\epsilon_{448}$ = 76 $mM^{-1}$ for the ferrous-CO complex of the enzyme. The ferric−cyanide hemoprotein complex was made by addition of 0.5 M KCN (dissolved in 1 M Tris-HCl, pH 7.8) to the sample immediately prior to recording of the absorbance spectrum (the sample pH was ~8.5 at the cyanide concentration used). Substrate perturbation difference spectra were performed as described previously (McMillan & Masters, 1993) employing arithmetic subtraction methods. Additions to samples resulted in total volume changes of ≤5%.

*Cytochrome c Reduction.* Electron transfer catalyzed by the NOS flavoproteins was monitored as NADPH-dependent cytochrome *c* reduction (Masters *et al.,* 1967) using the extinction coefficient $\epsilon_{550}$ = 21 $mM^{-1}$ (Massey, 1959). The 1.0-mL reaction mixtures contained 45 μM cytochrome *c* and 50 mM NADPH in 50 mM Na-Hepes buffer, pH 7.5, and experiments were conducted at 23 °C. Reactions were started by the addition of enzyme and monitored for 30−60 s. Measurement of cytochrome *c* reductase activity in cell extracts or partially purified flavoprotein solutions was made as described with the inclusion of 5 mM KCN in the assay mixture to inhibit cytochrome *c* reduction by bacterial cytochromes. Estimates of the amount of NOS flavoprotein present were made using the specific activity of the proteolytically derived NOS flavoprotein of 3−4 μmol/min/mg (Sheta *et al.,* 1994). Total protein was determined by the Bradford dye-binding assay using human serum albumin as a standard (Bradford, 1976).

*General Methods.* Immunoblot analysis of protein separated by electrophoresis on 10% SDS−polyacrylamide gels and transferred to nitrocellulose was performed using rabbit anti-rat neuronal NO synthase IgG and alkaline phosphatase-linked goat anti-rabbit IgG. Amino-terminal sequence analysis of the C1 flavoprotein (purified as described for C2) was performed by Edman degradation using an Applied Biosystems 477A sequencer. The protein was separated by SDS−polyacrylamide gel electrophoresis and transferred to poly(vinylidine difluoride) membrane by electroblot (Matsudaira, 1987). The immobilized protein band was excised and subjected to sequence analysis.

## RESULTS AND DISCUSSION

*Expression of the Hemoprotein.* The NO synthase hemoprotein, residues 1−714, was expressed in *E. coli* using the *tac* expression vector pCW. Figure 1 shows the presence of a soluble protein with the predicted molecular mass of 80 kDa, which was immunoreactive toward rabbit anti-rat neuronal NOS IgG. The partially purified hemoprotein elicited a reduced, CO difference spectrum with a wavelength maximum at 445 nm (Figure 2A) and spectral perturbation upon addition of L-arginine (Figure 2B) characterized by a 395-nm wavelength maximum and a 420-nm minimum in the difference spectrum (type I; McMillan & Masters, 1993). These properties indicate that the bacterially expressed hemoprotein possesses properties of the intact enzyme. Protein expression was estimated by CO difference spectroscopy to be ~100 nmol/L of induced culture. Purification of the hemoprotein by conventional chromatographic methods has been unsuccessful, with both loss of the heme prosthetic group and conversion of the ferrous-CO complex to a denatured 420-nm species. To facilitate protein purification, additional constructs which incorporate an amino-terminal alanine and four histidine residues have been prepared. The histidine track was added in order to utilize Ni-chelate chromatography in protein purification. The $His_4$-tagged hemoprotein, partially purified by Ni-NTA agarose chromatography, yielded ~7.5 nmol/L of induced culture (estimated from the Soret transition band absorbance of the imidazole−hemoprotein complex).

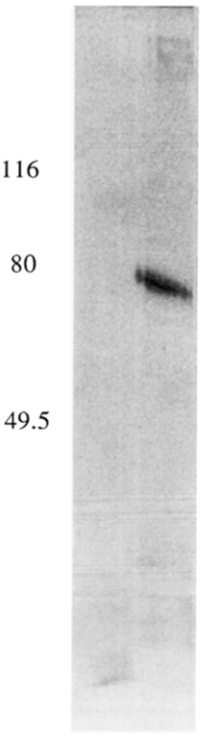


FIGURE 1: Immunoblot analysis of the NOS hemoprotein. The hemoprotein was partially purified by ammonium sulfate precipitation and Q Sepharose chromatography as described in Experimental Procedures, and an aliquot was subjected to SDS−PAGE (10% gel) and immunoblot analysis using rabbit anti-NOS IgG and alkaline phosphatase-linked goat anti-rabbit IgG. Prestained molecular mass markers (Bio-Rad) are 116 kDa, β-galacatosidase; 80 kDa, bovine serum albumin; and 49.5 kDa, ovalbumin.

*Site-Directed Mutagenesis of Cysteine-415.* The confirmation of the role of cysteine-415 in the axial ligation of the heme iron was made by mutagenesis to histidine. The identity of the histidine mutant hemoprotein, expressed as described above, was confirmed by immunoblot analysis and exhibits spectral properties consistent with incorporation of the heme prosthetic group. The absorbance spectra of the

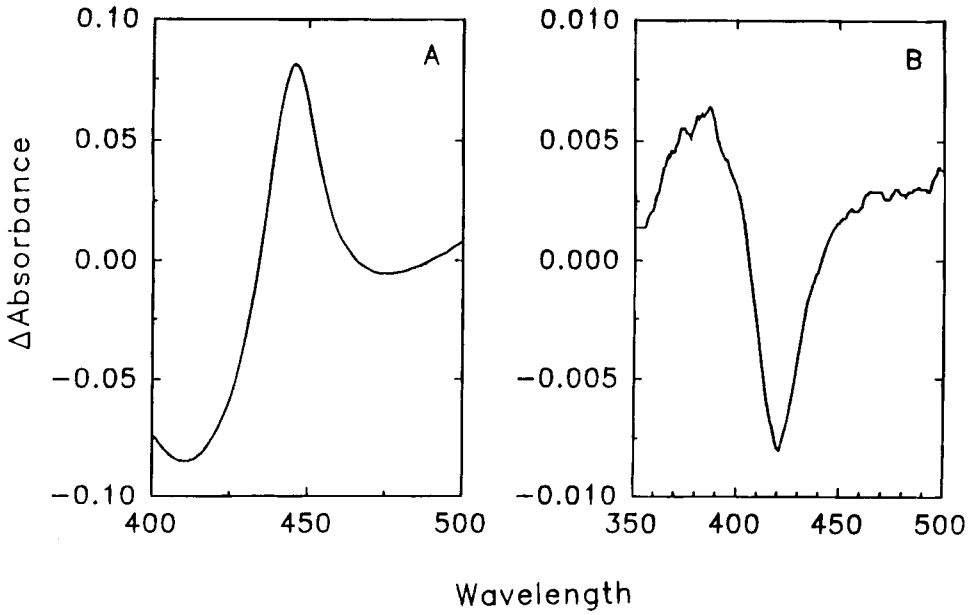


FIGURE 2: (Panel A) Carbon monoxide difference spectrum of the hemoprotein. The ferrous-CO complex of partially purified hemoprotein was prepared, and difference spectra were recorded as described in Experimental Procedures until the maximal absorbance difference ($A_{445}-A_{470}$) was obtained. (Panel B) L-Arginine spectral perturbation of the hemoprotein. The difference spectrum was recorded following the addition to the sample cuvette of L-arginine to a final concentration of 10 mM. The difference spectrum is a type I spectral perturbation, which is typical of difference spectra obtained with intact NOS upon addition of L-arginine.

imidazole-coordinated $His_4$-hemoproteins (100 mM imidazole), partially purified by Ni-NTA agarose chromatography, are shown in Figure 3A. The wild-type hemoprotein spectrum (curve A) exhibits wavelength maxima at 428, 544, and 575 nm representing the Soret, $\beta$, and $\alpha$ spectral transition bands, respectively, which are typical of the imidazole-induced absorbance of intact NOS (McMillan & Masters, 1993). The histidine mutant spectrum (curve B) exhibits wavelength maxima at 412, 530, and ~560 (shoulder) nm for the Soret, $\beta$, and $\alpha$ transition bands indicative of imidazole ligation at both the proximal and distal axial sites. The absorbance at 660 nm in both spectra is a charge-transfer band contributed by a residual high-spin component. The figure inset compares the visible spectra (5×) of the wild-type and mutant proteins. The bis-imidazole methemoglobin complex analogously exhibits wavelength maxima at 411, 534, and 560 nm (Brill & Williams, 1961). The thiolate proximal ligand of the heme iron has been shown to produce the ~450-nm Soret transition band of the ferrous-CO adduct in cytochromes P450 and chloroperoxidase (Omura & Sato, 1964; Dawson & Sono, 1987; Sono *et al.*, 1991), and replacement with an imidazole proximal ligand was predicted to shift the Soret band to ~420 nm. The ferrous-CO difference spectra of the wild-type and mutant hemoproteins dialyzed to remove imidazole are shown in Figure 3B. The wild-type hemoprotein (curve A) displays the characteristic wavelength maximum at 445 nm, with an absorbance excursion of 0.122 AU ($A_{445}-A_{470}$). The histidine mutant (curve B) exhibits a complete loss of the 445 nm absorbing ferrous-CO complex, developing a wavelength maximum at ~422 nm. The absorbance excursion ($A_{422}-A_{470}$) observed for the mutant ferrous-CO complex represents less than 10% of the total heme absorbance in the dialyzed sample. These data support the identification of cysteine-415 as the proximal heme ligand. Site-directed mutagenesis of the putative cysteine thiolate ligand of cytochrome $P450_d$ produced similar findings—an abolishment of the 450-nm ferrous-CO complex absorbance and a substoichiometric (~20% of wild-type 450-nm absorbance) 420 nm product (Shimizu *et al.*, 1988). Removal of the imidazole from the mutant NOS hemoprotein by dialysis resulted in denaturation of >90% of the protein, with essentially no loss of the heme chromophore. The dialyzed mutant hemoprotein (imidazole-free) was predominantly high-spin, as indicated by the 398-nm absorbance of the Soret transition band (data not shown), and was largely unresponsive to the addition of heme ligands, including imidazole, CO, and cyanide. These observations suggested stabilization of the mutant hemoprotein by imidazole, removal of which resulted in deformation of the heme-binding pocket. Wild-type protein handled under identical conditions did not exhibit this problem of instability, and all subsequent spectroscopic experiments (Figures 3–5) were conducted in the absence of imidazole (except the ferric-imidazole complex) using the same hemoprotein concentration.

*Additional Properties of the $His_4$-Hemoprotein.* The absorbance spectra of the ferric-cyanide complexes (20 mM KCN) of intact NOS (curve A) and the wild-type hemoprotein (curve B) are shown in Figure 4. The spectral properties of the hemoprotein ferric-cyanide complex are essentially identical to those of the intact enzyme, excepting absorbance that is attributable to the flavin prosthetic groups, providing further evidence for the integrity of the heme prosthetic group. The bands at 438 and 556 nm represent the Soret and $\beta/\alpha$ transitions, respectively, indicative of a thiolate proximal heme ligand. The ferric-cyanide complexes of cytochromes P450 were reported to exhibit a Soret transition band with an absorbance maximum at 439 nm (Dawson, 1988). The charge-transfer band at 650 nm can be attributed to residual high-spin component.

The L-arginine-binding spectra of the wild-type hemoprotein are shown in Figure 5. The protein is competent to bind L-arginine in the absence of exogenous $BH_4$ (curve A) as demonstrated by the type I difference spectrum upon addition of L-arginine to 100 $\mu$M. The dialyzed hemoprotein was low-spin, as indicated by the 420-nm absorbance

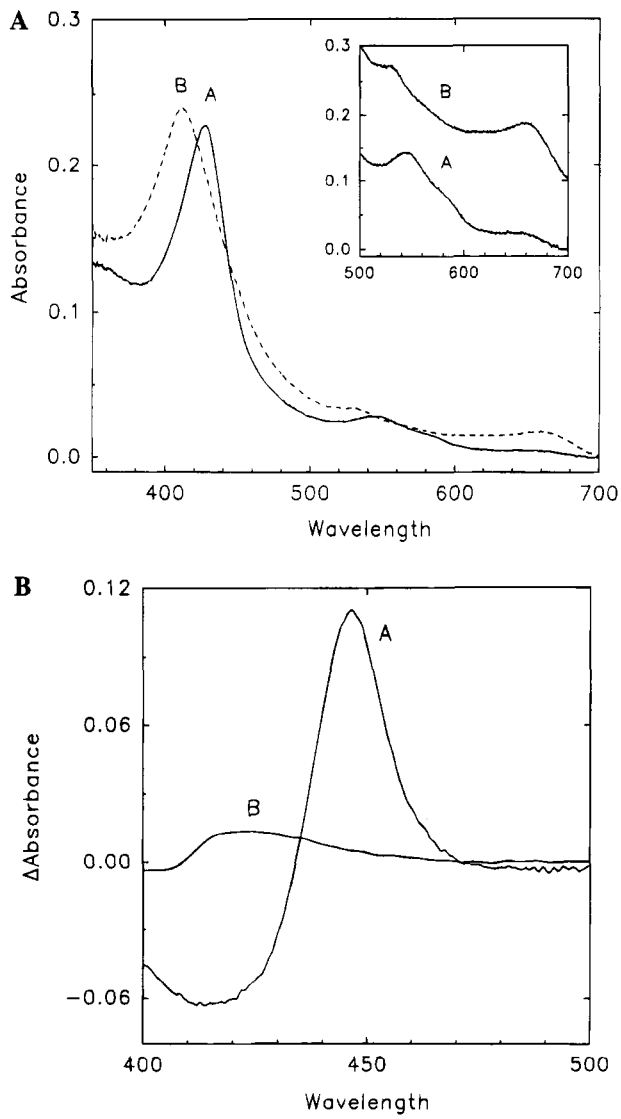


FIGURE 3: (Panel A) Absorbance spectra of the hemoprotein–imidazole complexes. The absorbance spectra of the wild-type (curve A) and $\Delta CH^{415}$ (curve B) $His_4$-hemoproteins, eluted from Ni-NTA agarose with 100 mM imidazole, are shown. The spectra shown in Figures 3–5 were obtained from the same wild-type or mutant $His_4$-hemoprotein preparations. The inset shows the visible spectra multiplied by a factor of 5 and offset by 0.1 AU for presentation. (Panel B) Ferrous-CO difference spectrum of the $His_4$-hemoproteins. The ferrous-CO complexes of the dialyzed wild-type (curve A) and $\Delta CH^{415}$ (curve B) hemoproteins, partially purified by Ni-NTA agarose chromatography, were prepared, and the difference spectra were recorded.

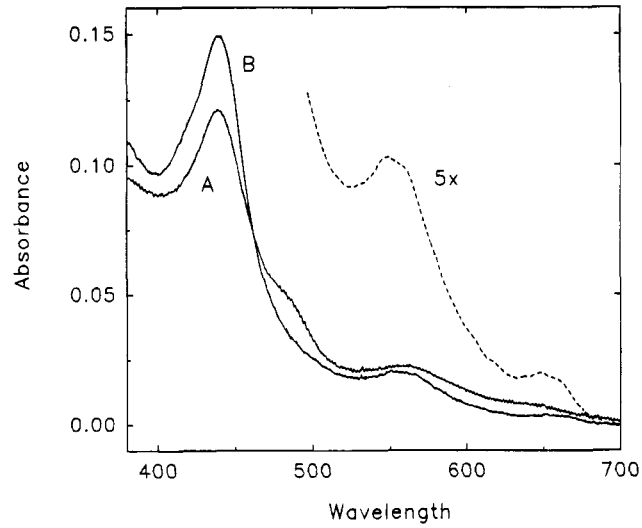


FIGURE 4: Absorbance spectra of intact NOS and hemoprotein ferric-cyanide complexes. The absorbance spectra of 3.3 mM intact NOS (curve A) and dialyzed wild-type $His_4$-hemoprotein (curve B) in the presence of 20 mM KCN are shown.

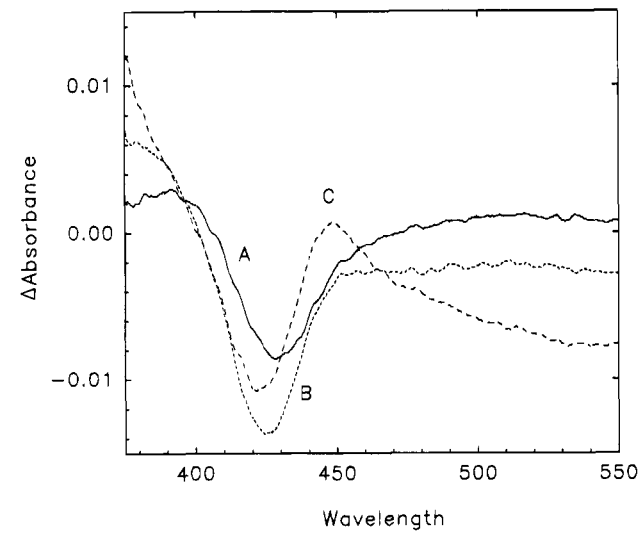


FIGURE 5: L-Arginine and $BH_4$ spectral perturbation of the $His_4$-hemoprotein. Spectra of the dialyzed wild-type hemoprotein were recorded in the presence and absence of 100 $\mu$M L-arginine, and the difference spectrum (curve A, solid line) was obtained by subtraction of the control spectrum from the perturbed spectrum. The effects of preincubation with 100 mM $BH_4$ for 20 min at 23 °C, in darkness, were examined. The difference spectra of the $BH_4$-preincubated samples perturbed by 100 mM L-arginine (curve B, long dashed line) and $BH_4$ alone (curve C, medium dashed line) were obtained by subtraction as described.

maximum of the Soret transition band (data not shown). The absorbance excursion ($A_{390}-A_{430}$) was 0.012 AU, which corresponded to ~10% of the hemoprotein as measured by formation of the ferrous-CO complex. Preincubation with 100 $\mu$M $BH_4$ for 20 min at 23 °C, followed by addition of 100 $\mu$M L-arginine, increased the absorbance change ($A_{390}-A_{420} = 0.02$) by ~2-fold (curve B). However, this increase was largely attributable to $BH_4$ alone, as shown in curve C. No effects on the ferrous-CO difference spectrum were observed. In other experiments (data not shown), the simultaneous incubation of dialyzed hemoprotein with 30 mM L-arginine and 0.5 mM $BH_4$ resulted in a 3-fold enhancement of the L-arginine spectral perturbation (over a 30-min incubation at 20 °C), in which the change in absorbance was approximately equal to that observed in the ferrous-CO difference spectrum. These data confirm the localization of the pterin-binding site to be within the amino-terminal half of the NOS molecule (on the amino-terminal side of the calmodulin-binding site) and furthermore indicate interaction between the pterin cofactor and the heme prosthetic group. The discrepancy between stoichiometries obtained from the L-arginine-induced spectral perturbation, the ferrous-CO complex formation, and the amount of total hemoprotein estimated from the absolute absorbance indicates that further efforts are required in the stabilization of this protein. The presence of bound nonproductive pterin derived from the heterologous expression system has been hypothesized on the basis of evidence described above. Immunoblot analysis showed the presence of degradation products that were immunoreactive toward anti-NOS IgG

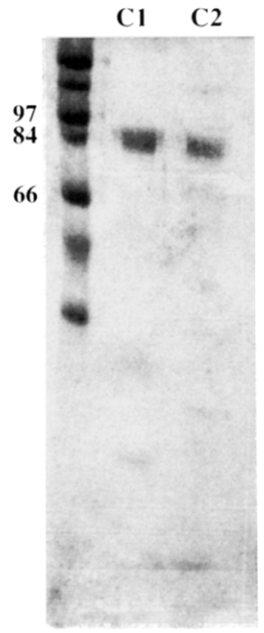


FIGURE 6: SDS−PAGE analysis of the NOS flavoproteins. The C1 flavoprotein was purified by 2′,5′-ADP Sepharose and calmodulin agarose affinity chromatography, and the C2 flavoprotein was purified by 2′,5′-ADP Sepharose, DEAE Sepharose, and Sephacryl 200 chromatographic methods as described in Experimental Procedures. Samples were analyzed by SDS−PAGE using a 10% gel. Molecular mass markers are 97 kDa, phosphorylase b; 84 kDa, fructose-6-phosphate kinase; and 66 kDa, bovine serum albumin.

and that presumably account for at least part of the observed inconsistencies. Elimination of the copurification of $His_4$-tagged degradation products will be attempted by expression of a carboxy-terminal histidine-tagged hemoprotein, which may also restore the considerably higher expression levels observed in the absence of the affinity tag.

*Expression and Characterization of the Flavoprotein Oxidoreductases.* The NOS flavoproteins C1 (residues 715−1429) and C2 (residues 750−1429) were expressed in *E. coli* using the *tac* expression vector pPROK-1. Expression levels were 12−25 nmol/L of induced culture for both proteins measured by cyanide-insensitive NADPH-dependent cytochrome *c* reduction. The proteins were partially purified from a soluble cell extract by 2′-ADP Sepharose 4B chromatography. NADPH (millimolar concentrations) has been employed previously in the elution of NOS from the 2′,5′-ADP Sepharose affinity medium by this group and other investigators. 2′-AMP was found not to elute NOS at concentrations up to 10 mM, except in the presence of 0.4 M NaCl. The C1 flavoprotein was subject to proteolytic degradation of the calmodulin-binding motif, as determined by amino-terminal sequence analysis, and <10% of the preparation was competent in binding $Ca^{2+}$/calmodulin. However, intact C1 flavoprotein was effectively purified by calmodulin affinity chromatography. SDS−PAGE analyses of the C1 and C2 flavoproteins, purified as described in Experimental Procedures, are shown in Figure 6.

The optical absorbance of the oxidized C2 flavoprotein, with wavelength maxima at 390 and 455 nm, characteristic of a flavin prosthetic group, is shown in Figure 7. The reduction of the flavoprotein with NADPH resulted in the formation of an air-stable semiquinone characterized by the increase in visible absorbance. The C2 flavoprotein exhibited NADPH-dependent cytochrome *c* reductase activity of 3−4

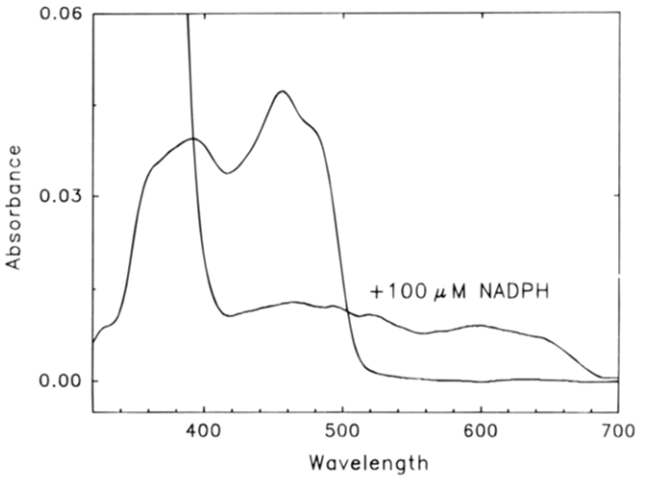


FIGURE 7: Absorbance spectrum of the C2 flavoprotein. The absorbance spectrum of the purified C2 flavoprotein was recorded after oxidation with potassium ferricyanide and desalting using Sephadex G50 and DTT-free buffer B. The spectrum exhibited wavelength maxima at 390 and 455 nm, which are attributable to absorbance of the flavin prosthetic groups. NADPH was added to a final concentration of 100 μM, and the spectrum was recorded.

Table 2: NADPH-Dependent Cytochrome *c* Reductase Activity

| flavoprotein | $Ca^{2+}$/CaM | TFP | EGTA | sp act.[a] |
|---|---|---|---|---|
| C1 | − | − | − | 2 |
| C1 | + | − | − | 4 |
| C1 | + | + | − | 2 |
| C1 | + | − | + | 2 |
| C2[b] | − | − | − | 3−4 |
| C2[b] | + | − | − | 3−4 |

[a] Specific activity: μmol/min/mg. [b] No effect of TFP or EGTA on cytochrome *c* reduction catalyzed by C2 was detected.

μmol/min/mg. The rate of NADPH-dependent cytochrome *c* reduction by the isolated NOS flavoproteins is 2−4-fold higher than in the intact enzyme in the absence of $Ca^{2+}$/calmodulin (McMillan *et al.,* 1992; Sheta *et al.,* 1994). This is in agreement with the rate of cytochrome *c* reduction observed for the proteolytically derived flavoprotein (Sheta *et al.,* 1994). Activation of the calmodulin-affinity-purified C1 flavoprotein by $Ca^{2+}$/calmodulin increased the rate of the cytochrome *c* reduction 2-fold. Addition of the chelator EGTA or the calmodulin antagonist trifluoperazine abolished the elevated rate of cytochrome reduction, indicating a calmodulin-specific activation of electron transfer; these results are summarized in Table 2. As a control, trifluoperazine or EGTA was added to C2 and no effect was seen on the rate of cytochrome *c* reduction (data not shown). The role of calmodulin in the regulation of NOS has been shown to be modulation of the flow of NADPH-derived electrons from the flavins to the heme iron reaction center (Abu-Soud & Stuehr, 1993). The effects observed for the isolated flavoprotein domain indicate that calmodulin binding can result in intradomain conformational changes in NOS (Sheta *et al.*, 1993; *vide infra*), as well as interdomain interaction of the heme-binding and flavoprotein domains, during electron transfer to the heme iron (Abu-Soud & Stuehr, 1993). The data reported herein also indicate that the binding site for calmodulin resides in the region of residues 715−750.

The complex nature and molecular size of NO synthases represent significant challenges to structural studies, and hence, the approach of dissection of the enzymes into

functional modules by molecular cloning has been undertaken. The findings that the heme/pterin-binding and flavoprotein domains are expressed as distinct polypeptides, with integral properties in a prokaryotic system, thus facilitating both culture conditions and genetic manipulations, demonstrate the utility of this approach. The L-arginine spectral perturbation, as well as preliminary radiolabeled $BH_4$- and L-arginine-binding measurements (conducted by Dr. Steven S. Gross), confirm the presence of the pterin-binding site within the amino-terminal half of neuronal NO synthase. Reconstitution of NO and citrulline formation or flavoprotein-mediated electron transfer to the hemoprotein have not yet been attempted and will be addressed in future studies. Also of interest is the potential of peroxide-mediated substrate oxygenation by the NOS hemoprotein. This introductory report verifies the position of the cysteinyl proximal ligand to the heme iron by site-directed mutagenesis, demonstration of pterin binding to the amino-terminal, heme-binding domain, and calmodulin modulation of electron transfer within the flavoprotein oxidoreductase domain. In conclusion, the use of the approach of molecular dissection will undoubtedly enhance the rate of progress in structural studies of NO synthases, including definition of the role of various functional modules within the enzymes, mechanistic studies, and potential resolution of tertiary structures.

## ACKNOWLEDGMENT

The authors wish to thank Dr. John Salerno (Rensselaer Polytechnic Institute, Troy, NY) for insight into the pterin-binding module of NOS and comments on the interpretation of the hemoprotein spectral data and Dr. Steven S. Gross (Cornell Medical College, New York, NY) for performing the radiolabeled pterin binding assays.

## REFERENCES

Abu-Soud, H. M., & Stuehr, D. J. (1993) *Proc. Natl. Acad. Sci. U.S.A. 90*, 10769−10772.
Boddupalli, S. S., Oster, T., Estabrook, R. W., & Peterson, J. A. (1992) *J. Biol. Chem. 267*, 10375−10380.
Bradford, M. M. (1976) *Anal. Biochem. 72*, 248−254.
Bredt, D. S., & Snyder, S. H. (1990) *Proc. Natl. Acad. Sci. U.S.A. 86*, 9030−9033.
Bredt, D. S., Ferris, C. D., & Snyder, S. H. (1992) *J. Biol. Chem. 267*, 10976−10981.
Bredt, D. S., Hwang, P. M., Glatt, C. E., Lowenstein, C., Reed, R. R., & Snyder, S. H. (1991) *Nature (London) 351*, 714−718.
Brill, A. S., & Williams, R. J. P. (1961) *Biochem. J. 78*, 246−253.
Cho, H. J., Xie, Q., Calaycay, J., Mumford, R. A., Swiderick, K. M., Lee, T. D., & Nathan, C. (1992) *J. Exp. Med. 176*, 599−604.
Dawson, J. H. (1988) *Science 240*, 433−439.
Dawson, J. H., & Sono, M. (1987) *Chem. Rev. 87*, 1255−1276.
Gegner, J. A., & Dahlquist, F. W. (1991) *Proc. Natl. Acad. Sci. U.S.A. 88*, 750−754.
Klatt, P., Schmidt, K., & Mayer, B. (1992) *Biochem. J. 288*, 15−17.
Kwon, N. S., Nathan, C. F., Gilker, C., Griffith, O. W., Mathews, D. E., & Stuehr, D. J. (1990) *J. Biol. Chem. 265*, 13442−13445.
Li, H., Darwish, K., & Poulos, T. L. (1991) *J. Biol. Chem. 266*, 11909−11914.
Massey, V. (1959) *Biochim. Biophys. Acta 34*, 255−256.
Masters, B. S. S., Williams, C. H., Jr., & Kamin, H. (1967) *Methods Enzymol. 10*, 565−573.
Matsudaira, P. T. (1987) *J. Biol. Chem. 262*, 10035−10040.
Mayer, B., Mathias, J., Heinzel, B., Werner, E. R., Wachter, H., Schultz, G., & Bohme, E. (1991) *FEBS Lett. 288*, 187−191.
McMillan, K., & Masters, B. S. S. (1993) *Biochemistry 32*, 9875−9880.
McMillan, K., Bredt, D. S., Hirsch, D. J., Snyder, S. H., Clark, J. E., & Masters, B. S. S. (1992) *Proc. Natl. Acad. Sci. U.S.A. 89*, 11141−11145.
Michael, S. F. (1994) *Biotechniques 16*, 410−412.
Narhi, L. O., & Fulco, A. J. (1987) *J. Biol. Chem. 262*, 6683−6690.
Omura, T., & Sato, R. (1964) *J. Biol. Chem. 239*, 2370−2378.
Pollock, J. S., Förstermann, U., Mitchell, J. A., Warner, T. D., Schmidt, H. H. H. W., Nakane, M., & Murad, F. (1991) *Proc. Natl. Acad. Sci. U.S.A. 88*, 10480−10484.
Ravichandran, K. G., Boddupalli, S. S., Hasemann, C. A., Peterson, J. A., & Deisenhofer, J. (1993) *Science 261*, 731−736.
Salerno, J. C., & Morales, A. J. (1994) *Biochemistry and Molecular Biology of Nitric Oxide, First International Conference* (Ignarro, L., and Murad, F., Eds.) p 72, UCLA, Los Angeles, CA.
Sheta, E. A., McMillan, K., & Masters, B. S. S. (1994) *J. Biol. Chem. 269*, 15147−15153.
Shimizu, T., Hirano, K., Takahashi, M., Hatano, M., & Fujii-Kuriyama, Y. (1988) *Biochemistry 27*, 4138−4141.
Sono, M., Hager, L. P., & Dawson, J. H. (1991) *Biochim. Biophys. Acta 1078*, 351−359.
Stuehr, D. J., & Ikeda-Saito, M. (1992) *J. Biol. Chem. 267*, 20547−20550.
Stuehr, D. J., Cho, H. J., Kwon, N. S., Weise, M. F., & Nathan, C. F. (1991) *Proc. Natl. Acad. Sci. U.S.A. 88*, 7773−7777.
Vorherr, T., Knopfel, L., Hofmann, F., Mollner, S., Pfeuffer, T., & Carafoli, E. (1993) *Biochemistry 32*, 6081−6088.
White, K. A., & Marletta, M. A. (1992) *Biochemistry 31*, 6627−6631.

BI942090O